Kinetics of the Interaction between DNA and Acridine Orange

Naohisa KURE, Takayuki SANO,* Shoji HARADA, and Tatsuya YASUNAGA
Department of Materials Science, Faculty of Science, Hiroshima University, Hiroshima 730
(Received July 14, 1987)

Both static and kinetic investigations have been performed on the interaction of calf thymus DNA with Acridine Orange (AO). The binding isotherm obtained spectrophotometrically was analyzed by a site exclusion theory and revealed the presence of two binding modes of dye molecule corresponding to intercalation and dimerization on DNA. In the kinetic experiments focusing on the intercalation mode by the temperature-jump technique, three relaxations were observed. From the analyses of both the relaxation time and amplitude, the two fast relaxations were ascribed to parallel binding reactions including a bimolecular pathway for direct transfer of dye molecule on the polymer and the slow relaxation was attributable to a conformational change of DNA molecules. The binding parameters kinetically obtained suggest that 80% of bound AO is in intercalated form and the remainder is in partially intercalated one as an external bound form.

The interaction of acridine dyes with deoxyribonucleic acid (DNA) has been extensively studied because of their wide biological activities.[1-5] Acridine dyes have two binding modes on DNA with different affinities. Most experiments have been focused on the strong binding mode which has been related to the biological activity of the dyes, and elucidated that this binding mode structurally corresponds to an intercalation of dye between two adjacent base pairs of DNA.[6-12]

The stoichiometry of the binding of acridine dyes to DNA has been investigated by equilibrium dialysis[13-19] and/or visible spectroscopy.[13,20-22] The affinity of the intercalation mode has been found firstly to be independent of the base composition of DNA.[13,20,21] For this reason, various static and kinetic models have been proposed on the assumption of homogeneous DNA sites for the binding of acridine dyes.[16,23-27] However, the heterogeneity of the binding site has been pointed out from the fluorescence studies on several acridine dye-DNA complexes.[28-36] Given these circumstances, the investigation on more fundamental nature of the binding through the reexamination of the proposed binding models are desirable. For this purpose, Acridine Orange (AO) would be most favorable since this dye is known to form the intercalative complex independent of the base specificity of DNA.[32,33,35,37]

In this paper, thus the interaction between AO and calf thymus DNA focusing on the intercalative binding mode was studied by visible spectrophotometry and temperature-jump spectroscopy. A basic nature of the binding mechanism of acridine dyes with double stranded DNA was also discussed.

Experimental

Calf thymus DNA (sodium salt, type I) was purchased from Sigma Chemical Company and purified twice by phenol extraction. The hyperchromicity on thermal denaturation at 260 nm was 37—38% at pH 6.5 in the 1 mM† phosphate buffer. The concentration of DNA was determined using ε_{260}=6600 M^{-1} cm^{-1} per nucleotide. Acridine Orange (AO) was purchased from Eastman Kodak Company and was recrystallized twice as the base from a solution of Acridine Orange hydrochloride in a 1:1 water–ethanol mixture. The concentration of AO was determined spectrophotometrically at 492 nm by using the molar extinction coefficient proposed by Stone and Bradley.[38] Other chemicals used were reagent grade. All sample solutions were prepared in lmM phosphate buffer containing 0.2 M sodium chloride at pH 6.5.

Absorption spectra were measured with a Union Giken SM 401 spectrophotometer. Kinetic measurements were performed using the joule heating temperature-jump apparatus of which detail has been described elsewhere.[39] The light source was a halogen lamp (250 W) and the path length of the cell was 10 mm. The rise time and magnitude of the temperature-jump were about 10 μs and 7 °C, respectively. The orientational effect of DNA was canceled out by placing the polarizer between the cell and the monochromator.

All the static and kinetic measurements were performed at 25.0±0.2 °C. The data were analyzed on the basis of the neighbor exclusion model established by McGhee and von Hippel.[40]

Results

Binding Isotherm. The visible absorption spectra of AO–DNA complexes at various P/D (the ratio of DNA phosphate to dye) values in 0.2 M NaCl solution displayed an isosbestic point at 496 nm, in agreement with the results reported by Fredericq and Houssier.[17] They tried to obtain a binding isotherm from spectral shifts using the absorbance at 465 nm, but failed to obtain the consistent results with the equilibrium dialysis ones. This discrepancy in the binding data seems to come from the fact that molar extinction coefficient at 465 nm of bound AO varies significantly depending on the binding ratio r (bound AO/DNA phosphate).

In the present study, the binding isotherm was determined spectrophotometrically using the absorbance at 492 nm since the molar extinction coefficient on bound AO at this wavelength was reported to be

† 1 M=1 mol dm^{-3}.

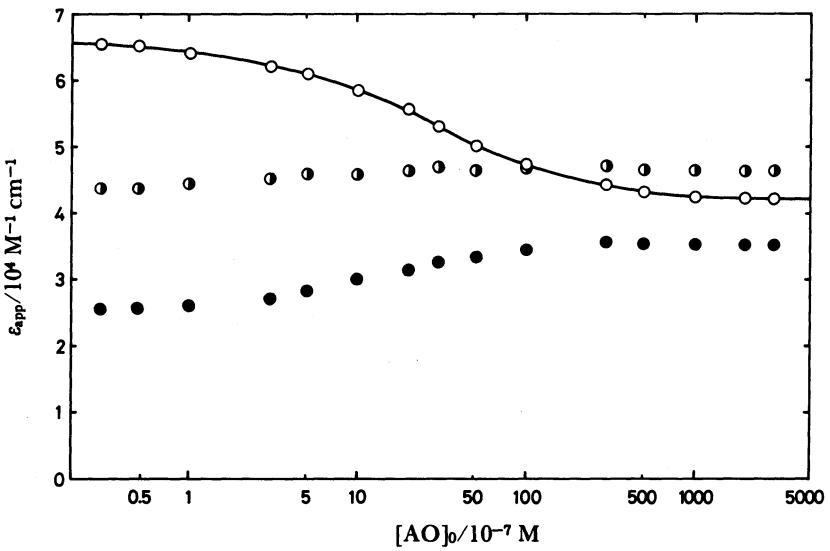

Fig. 1. Change in apparent molar extinction coefficient (ε_{app}) of AO-DNA solution with increasing AO concentration at a fixed P/D of 10 and 25 °C: (O), at 492 nm; (O), at 504 nm; (●), at 510 nm.

invariant for r below 0.2.[16] The apparent molar extinction coefficient (ε_{app}) of AO-DNA solutions were measured at various AO concentrations from 3×10^{-8} M to 3×10^{-4} M by holding P/D equal to 10, and represented in Fig. 1. In the solution of AO alone, generally, the dimerization equilibrium of the dye must exist. But in the system involving DNA under the present experimental condition of $r<0.2$, the contribution of dimeric species to the free AO molecule is less than 5%. Consequently, in the present analyses, the free AO molecule was regarded as all monomeric species. From the lower and higher limits of concentration in this figure, the extinction coefficients at 492 nm were obtained to be $\varepsilon_f=66000$ $M^{-1}cm^{-1}$ for free AO and $\varepsilon_b=42000\ M^{-1}cm^{-1}$ for bound AO, respectively. The concentration of free dye, A, and the binding ratio, r, were determined from the next equations:

$$A=\frac{\varepsilon_{app}-\varepsilon_b}{\varepsilon_f-\varepsilon_b}A_0 \tag{1}$$

$$r=\frac{A_0-A}{P_0} \tag{2}$$

where A_0 and P_0 are the total concentrations of AO and DNA (in phosphate unit), respectively. In Fig. 2, a Scatchard plot using these equations was illustrated together with those obtained from equilibrium dialysis experiments by Armstrong et al.,[16] and Fredericq et al.[17] A good agreement between these isotherms suggests the validity of the spectrophotometrical method employed in this study.

The obtained binding isotherm was analyzed by considering a dimeric species formed by an additional

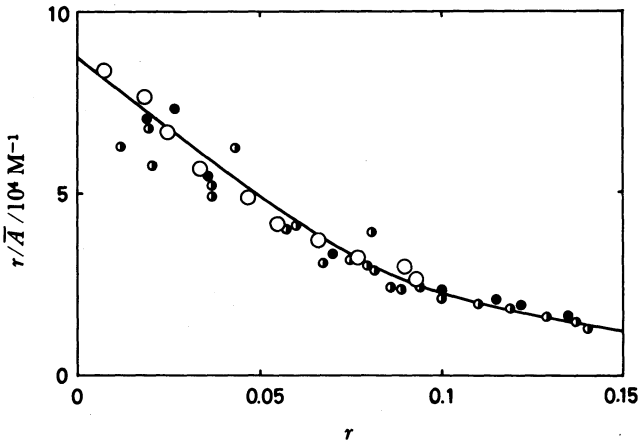

Fig. 2. Scatchard plots of binding of AO to DNA at 25 °C: (O), obtained from the present spectrophotometrical method in 0.2 M NaCl solution; (●), by Armstrong et al.,[16] in 0.2 M NaCl solution; (◑), by Fredericq and Houssier[17] in 0.1 M NaCl solution. The solid line shows the theoretical curve calculated using $n=3$, $K_I=1.8\times10^5\ M^{-1}$, and $K_D=3\times10^4\ M^{-1}$.

binding of free dye to bound dye on DNA reported by Armstrong et al.[16] The Scatchard equation, based on the site exclusion theory including such dimerization mode was reported to be[19]

$$\frac{r}{\bar{A}}=\frac{K_I}{2}\frac{\{(1-2nr)+2K_D\bar{A}(1-nr)\}^n}{\{[1-2(n-1)r]+2K_D\bar{A}[1-(n-1)r]\}^{n-1}} \tag{3}$$

where K_I, K_D, n, and the overbar refer to the binding constant for intercalation, that of dimerization on the polymer, the number of sites blocked by one bound

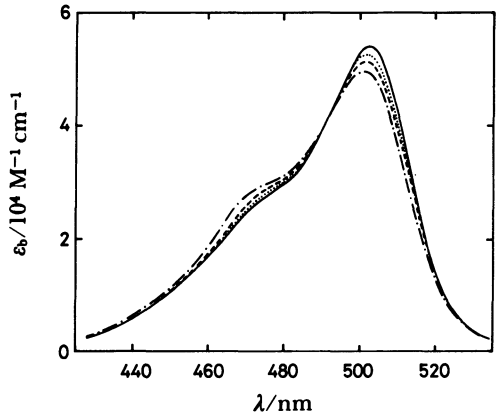

Fig. 3. Absorption spectra of AO-DNA complexes in 0.2 M NaCl solution at various values of binding ratio r: (——), r=0.01; (……), r=0.032; (---), r=0.045; (—·—), r=0.076. The total dye concentration is 10^{-5} M.

dye, and the equilibrium concentration, respectively. The analysis of the binding isotherm using this equation yields the following binding parameters: K_I=1.8×10^5 M^{-1}, K_D=3×10^4 M^{-1}, and n=3. As can be seen in Fig. 2, all observed data fall on the theoretical curve calculated using these values within an experimental uncertainty. These results are consistent with the assignment of the binding isotherm to the intercalation and dimerization modes.

Spectral Properties of Intercalated AO. In order to examine the spectral properties of intercalative species, the absorption spectra of AO-DNA complex were measured for P/D values above 10 at constant DNA concentration, where the contribution of bound dimer species is negligibly small (estimated from the values of K_I and K_D). Figure 3 illustrates the spectra of bound dye molecules obtained by a substraction of the contribution of free dye. As judged from the figure, an absorption peak at longer wavelength is progressively depressed and a shoulder at shorter one increases gradually with binding. This kind of spectral behavior has been reported as characteristics of AO-AO interactions on polymers.[41] Since the bound dimer species is negligible under the present experimental condition of r<0.1, the observed spectral variation would be attributable to the interaction between monomeric intercalated AO molecules. This assignment is supported by other optical properties of bound AO observed in the corresponding range of r, e.g., fluorescence depolarization[17,35] and exciton splitting in circular dichroism.[17,42,43]

As an additional remark, it should be noted that the constant absorbance at 492 nm of bound AO in Fig. 3, led us to using of this wavelength to obtain the binding isotherm in the preceding section.

Characteristics of Relaxation. Since our primary attention is the intercalation mechanism, the temperature-jump measurements were performed in the range of r below 0.1. An instantaneous and small absorbance change, beyond the resolution time of the apparatus, was followed by three distinguishable relaxation processes as shown in Figs. 4a and 4b. These three processes are named fast, middle and slow processes in order of the time region fast to slow. The relaxation amplitudes of these relaxations are represented in Fig. 5. As shown in Fig. 5a, the spectra of relaxation amplitudes of the fast and middle processes are well correlated to the difference spectrum between free AO and intercalated AO (the difference spectrum was illustrated using the extinction coefficients in Fig. 1). On the other hand, as shown in Fig. 5b, the spectrum of relaxation amplitude of the slow process is quite similar to the difference spectra between intercalated AO at different binding ratios (the difference spectra were obtained from the spectra in Fig. 3).

To see the reaction mechanism in more detail two kinds of concentration dependence of the reciprocal relaxation times were measured for each process: Figure 6 shows their concentration dependences at

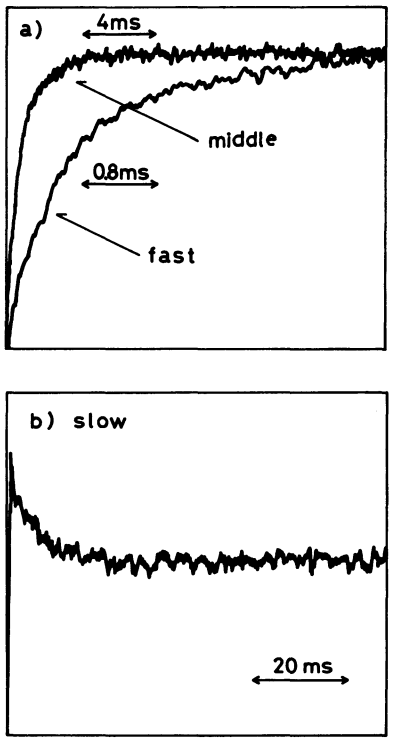

Fig. 4. Typical relaxation curves observed for AO-DNA system in 0.2 M NaCl solution at 480 nm (absorbance increasing upward): (a), fast and middle process, [AO]=1.0×10^{-5} M and [DNA]-phosphate=1.0×10^{-5} M; (b), slow process observed by averaging 4 repetitions, [AO]=3.0×10^{-5} M and [DNA]phosphate=9×10^{-4} M. The final temperature is 25 °C.

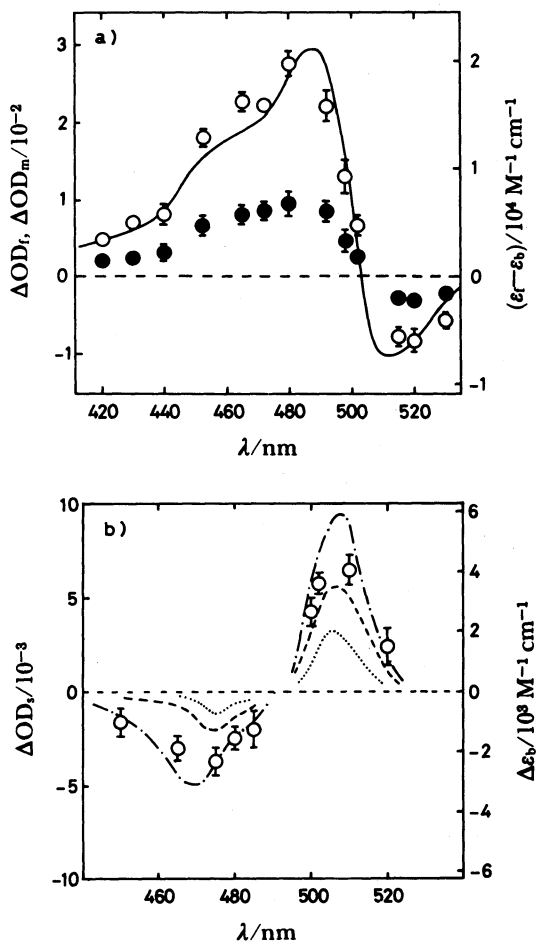

Fig. 5. Wavelength depedence of relaxation amplitude of each process. (a) , (○) and (●) represent the experimental values of ΔOD_f and ΔOD_m, respectively, at [AO]=1.0×10^{-5} M and [DNA]phosphate=1.0×10^{-4} M. The solid curve shows the difference spectrum between free and intercalated AO ($\varepsilon_f-\varepsilon_b$). (b), (○) represents the experimental values of ΔOD_s at [AO]=5×10^{-3} M and [DNA]phosphate=1.5×10^{-3} M. The curves show the difference spectra between intercalated AO at different values of r: (—·—), $\varepsilon_b^{0.01}-\varepsilon_b^{0.076}$; (---), $\varepsilon_b^{0.01}-\varepsilon_b^{0.045}$, (·····), $\varepsilon_b^{0.01}-\varepsilon_b^{0.032}$, where superscripts refer to binding ratio.

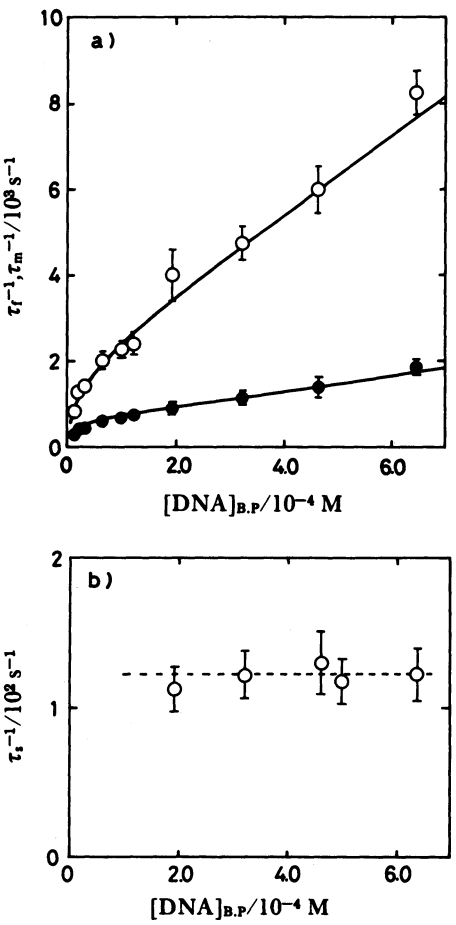

Fig. 6. Dependence of the reciprocal relaxation time of each process on total DNA concentration (base pairs unit) at P/D=10: (a), fast (○) and middle (●) processes, solid lines show the theoretical curves calculated from Eqs. 4 and 5 with constants listed in Table 1; (b), slow processes.

constant P/D=10; Fig. 7 shows the AO concentration dependences at 5×10^{-5} M of DNA (in base pairs unit) in the range of P/D≧10. As judged from Figs. 6a and 7a, the relaxation times of the fast and middle processes τ_f and τ_m are close to each other and both the relaxation times show similar dependences against DNA and AO concentration, respectively. While, the slow processes and the reciprocal relaxation time τ_s^{-1} displays no dependence on either DNA and AO concentrations (Figs. 6b and 7b).

Reaction Mechanism. The following three kinetic models have been proposed for the binding of several acridine and/or phenanthridine dyes to DNA on the assumption of homogeneity of intercalation sites:

$$A + S \underset{}{\overset{K_1}{\rightleftharpoons}} C, \qquad \text{(I)}$$

$$A + S \overset{K_1}{\rightleftharpoons} C_1 \overset{K_2}{\rightleftharpoons} C_2, \qquad \text{(II)}$$

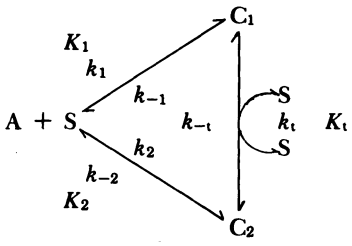

(III)

where A, S, and C_i denote free dye molecule, free site, and bound species, respectively; K_i, k_i, and k_{-i} (i=1, 2, and t) are the equilibrium constant, forward and backward rate constants in each process, respectively. Model I represents a simple bimolecular binding which has been proposed for ethidium-poly[d(A-T)] system.[44] Model II is a two-step binding model which

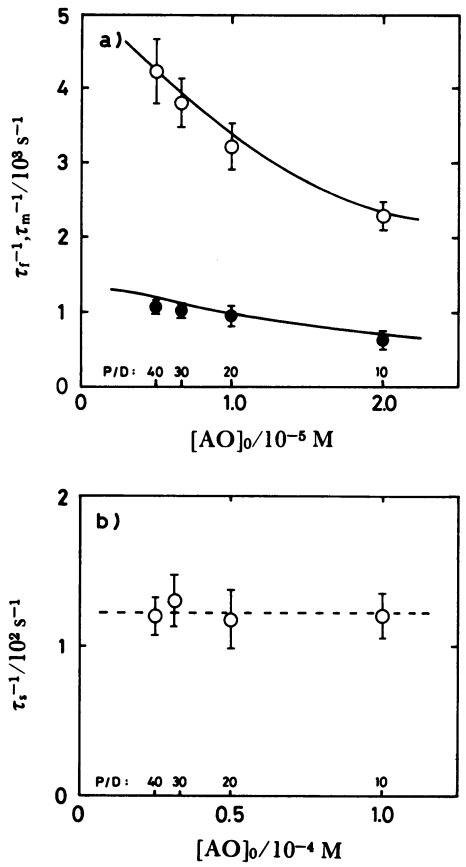

Fig. 7. Dependence of the reciprocal relaxation time of each process on total AO concentration at a constant DNA concentration: (a), fast (○) and middle (●) processes, solid lines show the theoretical curves calculated from Eqs. 4 and 5 with constants listed in Table 1; (b), slow process.

has been proposed for proflavine–DNA[23] and poly(A)–poly(U)[45] systems. The binding of AO to DNA has been interpreted by this model for the earlier studies using stopped-flow technique.[24,25] While Model III was originally proposed for ethidium–DNA system[26] and subsequently reported for several phenanthridine dyes and 10-methyl-9-aminoacridine.[27] The present kinetic data obtained for AO–DNA system were examined in detail for these three kinetic models.

(i) Fast and Middle Processes. At first, the fast and middle processes are analyzed since these are closely coupled and sufficiently faster than slow one. Among the kinetic models above, Model I of a single step reaction process can firstly be excluded from possible one. Secondarily, the concentration dependences of relaxation times calculated for Model II were quite different from the present observation. This fact also eliminated the Model II. Finally, Model III is examined. By an application of site exclusion theory, the kinetic analyses for this cyclic model give two relaxation times corresponding to the fast and middle processes (see Appendix A):

$$\tau_f^{-1} = \frac{1}{2}\{a_{11} + a_{22} + \sqrt{(a_{11}-a_{22})^2 + 4a_{12}a_{21}}\} \tag{4}$$

$$\tau_m^{-1} = \frac{1}{2}\{a_{11} + a_{22} - \sqrt{(a_{11}-a_{22})^2 + 4a_{12}a_{21}}\} \tag{5}$$

with

$$a_{11} = k_1(S_0 f(r) - \bar{A} f'(r)) + k_{-1} + k_t(S_0 f(r) + \bar{C}_1 f'(r)) - k_{-t}\bar{C}_2 f'(r), \tag{6}$$

$$a_{12} = k_1(S_0 f(r) - \bar{A} f'(r)) + k_t \bar{C}_1 f'(r) - k_{-t}(S_0 f(r) + \bar{C}_2 f'(r)), \tag{7}$$

$$a_{21} = k_2(S_0 f(r) - \bar{A} f'(r)) - k_t(S_0 f(r) + \bar{C}_1 f'(r)) + k_{-t}\bar{C}_2 f'(r), \tag{8}$$

and

$$a_{22} = k_2(S_0 f(r) - \bar{A} f'(r)) + k_{-2} - k_t \bar{C}_1 f'(r) + k_{-t}(S_0 f(r) + \bar{C}_2 f'(r)), \tag{9}$$

where S_0 and r denote the total concentration of binding site and the ratio of the bound dye to the total number of binding site, i.e., $r=(\bar{C}_1+\bar{C}_2)/S_0$, respectively; $f(r)$ and its derivative $f'(r)$ are the correction functions due to site exclusion and have the following general forms[44]

$$f(r) = \frac{(1-nr)^n}{\{1-(n-1)r\}^{n-1}} \tag{10}$$

$$f'(r) = \frac{\{(n-1)nr - 2n + 1\}(1-nr)^{n-1}}{\{1-(n-1)r\}^n} \tag{11}$$

The cyclic reaction of this model gives a relationship between six rate constants:

$$\frac{k_2}{k_{-2}} = \frac{k_1}{k_{-1}} \cdot \frac{k_t}{k_{-t}} \tag{12}$$

Seven unknown parameters (six rate constants and n) are involved in these equations. The analyses of τ_f^{-1} and τ_m^{-1} by a successive approximation method yield both $n=3$ and various sets of values for six rate constants which give the theoretical curves interpreting nicely all experimental data. However, a unique value for each rate constant could not be determined from this analysis. Accordingly, in order to determine unique values of six rate constants, the relaxation amplitudes of the fast and middle processes, ΔOD_f and ΔOD_m, were also examined on the basis of Model III. The relaxation amplitudes of ΔOD_f, ΔOD_m, and their ratio of $\Delta OD_f/\Delta OD_m$ are given by

$$\Delta OD_f = \frac{(\varepsilon_1 - \varepsilon_f) - (\varepsilon_2 - \varepsilon_f)\beta_m}{\beta_f - \beta_m} y_f^0, \tag{13}$$

$$\Delta OD_m = -\frac{(\varepsilon_1-\varepsilon_f)-(\varepsilon_2-\varepsilon_f)\beta_f}{\beta_f-\beta_m} y_m^0, \quad (14)$$

$$\frac{\Delta OD_f}{\Delta OD_m} = -\frac{(\varepsilon_1-\varepsilon_f)-(\varepsilon_2-\varepsilon_f)\beta_m y_f^0}{(\varepsilon_1-\varepsilon_f)-(\varepsilon_2-\varepsilon_f)\beta_f y_m^0}, \quad (15)$$

with

$$y_{f,m}^0 = \bar{A}\bar{S}\{\beta_{f,m}+\alpha K_1K_2+(1+\beta_{f,m})(1-\alpha)K_2(\bar{S}-\bar{A}f'(r))\}\delta K_1/\{1+(K_1+K_2)(\bar{S}-\bar{A}f'(r))\} \quad (16)$$

$$\beta_{f,m} = (\tau^{-1}{}_{f,m}-a_{22})/a_{12} \quad (17)$$

$$\alpha = \Delta H_2/\Delta H_1 = (\delta K_2/\delta K_1)(K_1/K_2), \quad (18)$$

where ε_f, ε_i, ΔH_i, and δK_i (i=1,2) denote the molar extinction coefficient of free AO, that of complex C_i, the standard enthalpies, and equilibrium shifts by the temperature-jump in process i, respectively. The derivation of these equations are shown in Appendix B. As can be seen from Fig. 5a, the wavelength dependences of ΔOD_f and ΔOD_m are not only quite similar each other, but both are well correlated with the difference spectrum between free and bound AO. Further, the value of $\Delta OD_f/\Delta OD_m$ calculated using the data in Fig. 5a is constant against wavelength within an experimental uncertainty as shown in Fig. 8. These experimental results require that both ΔOD_f and ΔOD_m in Eqs. 13 and 14 should be proportional to $(\varepsilon_b-\varepsilon_f)$, and that the representation of Eq. 15 for $\Delta OD_f/\Delta OD_m$ should be independent of wavelength. To satisfy these requirements, any one of the following three relationships among ε_1, ε_2, ε_f, and ε_b must be hold at every wavelengths: (a) $\varepsilon_1=\varepsilon_2=\varepsilon_b$, (b) $\varepsilon_1=\varepsilon_f$ and $\varepsilon_2=\varepsilon_b$, and (c) $\varepsilon_1=\varepsilon_b$ and $\varepsilon_2=\varepsilon_f$. Thus, the concentration dependences of $\Delta OD_f/\Delta OD_m$ was analyzed in detail using Eq. 15 for the cases (a), (b), and (c), respectively. In the cases of (a), (b), however, calculated values of $\Delta OD_f/\Delta OD_m$ were quite different from the experimental data. In the case of (c), Eq. 15 can be simplified as

$$\left(\frac{\Delta OD_f}{\Delta OD_m}\right)_c = -\frac{y_f^0}{y_m^0}, \quad (19)$$

where subscript c refer to the case (c). The analysis using this equation for the various values for α and rate constants obtained above yields α=0.9±0.1, n=3, and unique set of rate constants listed in Table 1, which fully satisfy all the experimental data. As shown in Fig. 9, a plot of $\Delta OD_f/\Delta OD_m$ measured versus $(\Delta OD_f/\Delta OD_m)_c$ calculated using the obtained parameters showed an excellent fitting. The all observed data of τ_f^{-1} and τ_m^{-1} fall on the theoretical curves calculated, for the same parameters, using Eqs. 4 and 5 as can be seen from Figs. 6a and 7a. These agreements confirm the plausibility of Model III as well as the equivalence in spectral behaviors of species C_1 with the bound AO and C_2 with the free AO.

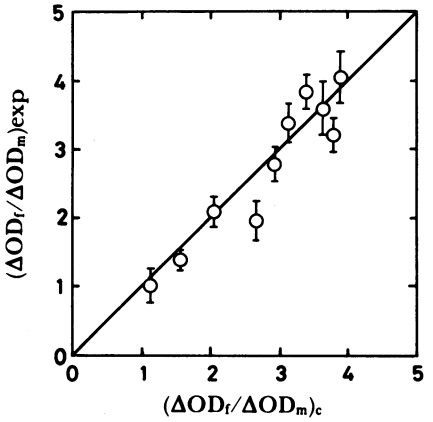

Fig. 9. A plot of $\Delta OD_f/\Delta OD_m$ obtained experimentally at various concentrations vs. $(\Delta OD_f/\Delta OD_m)_c$ calculated from Eq. 19 using parameters listed in Table 1.

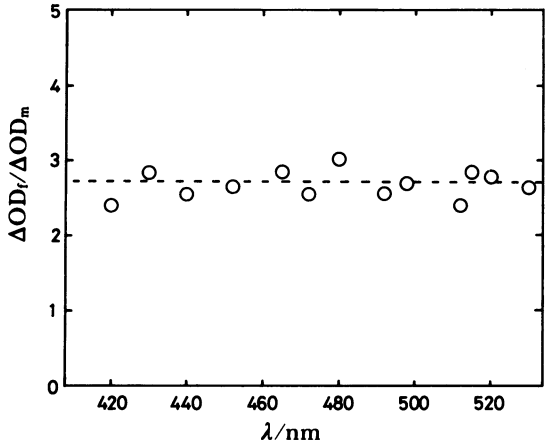

Fig. 8. Wavelength dependence of the experimental values of the relative amplitude $\Delta OD_f/\Delta OD_m$, obtained using the data in Fig. 5a.

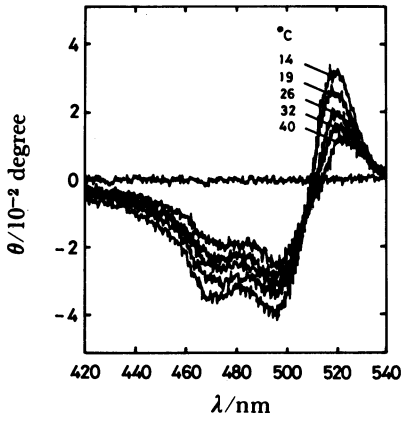

Fig. 10. CD spectra of AO in the presence of DNA in 0.2 M NaCl solution at various temperature in the premelt range. [AO]=3.3×10^{-5} M, [DNA]-phosphate=6.6×10^{-4} M (P/D=20).

Furthermore, the value of $n=3$ determined kinetically is identical with the value obtained from the analysis of the binding isoterm. The overall binding constant, $K_1+K_2=(1.6\pm0.3)\times10^5\ M^{-1}$, calculated from the obtained rate constants is nicely consistent with the binding constant for intercalation mode, $K_I=1.8\times10^5\ M^{-1}$, determined statically. These facts give further confidence for the present assignment.

(ii) Slow Process. As can be seen from Fig. 5b, the spectrum of the relaxation amplitude of the slow process is well associated with the spectral variations resulting from the interaction between intercalated AO molecules. To see this point further, the CD spectra of AO-DNA complex, which is sensitive to dye-dye interactions, were measured at P/D=20 as a function of temperature in the premelt range. As shown in Fig. 10, the exciton splitting due to intercalated AO-AO interaction[17,44] was observed, and decreased with elevation of temperature. Since the amount of bound dye can be regarded as approximately constant in this temperature range,[15,18] this CD shift clearly demonstrates that the interaction between intercalated dyes depends considerably on temperature. Furthermore, the direction of CD shift indicates that this interaction successively weaken with temperature increase. This is compatible with the direction of the relaxation observed by temperature-jump measurements. The slow relaxation process is thus attributable to intercalated AO-AO interaction which depends on temperature.

By the way, the strength of interaction between the intercalated dye molecules depends strongly on both the distance and angle between the interacting dye molecules.[46] In the case of intercalating dyes, these stereochemical parameters would be determined by the double helical structure of DNA. Therefore, the present relaxation seems to result from a thermally induced configurational alternation of DNA molecule itself, which brings about the changes on the steteochemical relationship between intercalated AO molecules. In the case that this configurational alternation arises from an equilibrium shift between two states of DNA structure, the reaction scheme for this process may be represented by the following simple form independent of the fast two relaxations:

$$[\mathrm{DNA}]_X \underset{k_{-3}}{\overset{k_3}{\rightleftarrows}} [\mathrm{DNA}]_Y, \qquad \text{(IV)}$$

where $[DNA]_X$, $[DNA]_Y$, k_3, and k_{-3} denote the two states of DNA structure named X and Y, the forward and backward rare constants, respectively. The equation of the reciprocal relaxation time, τ_3^{-1}, is given by

$$\tau_3^{-1} = k_3 + k_{-3}, \qquad (20)$$

where the relaxation time is essentially independent of DNA and AO concentrations, which is consistent with the experimental results as seen in Figs. 6b and 7b. By averaging the experimental values of τ_3^{-1}, k_3+k_{-3} was obtained to be $120\pm10\ s^{-1}$. The states X and Y introduced above can not be identified in the present study. However, these may be associated with the thermally induced premelt transition of DNA which has been demonstrated by CD spectroscopies[47,48] and NMR studies.[49]

When the whole results are reviewed, it should be noted that the only faster two of three relaxations were assigned to the actual interactions between AO and DNA molecules. This is consistent with the fact that the overall association constant K_1+K_2 determined kinetically for the two fast relaxations agrees well with the binding constant K_I estimated statically.

Discussion

Intercalating Species. The present kinetic results elucidated the presence of two types of bound dye species (C_1 and C_2) in the range of $r<0.1$. The values of binding constants for these species, K_1 and K_2, listed in Table 1 indicate that more than 80% of bound AO is in complex form C_1. In addition, the absorption spectrum of C_1 determined from the analyses of the relaxation amplitude is approximately identical with that of statically observed intercalated AO. These results strongly suggest that the species C_1 is attributable to the intercalative species.

The values of rate constants for the formation of complex C_1 can be compared to those reported for other intercalating dyes, and for a nonintercalating dye. The present results of $k_1=(3.4\pm0.2)\times10^7\ M^{-1}\ s^{-1}$

Table 1. Kinetic and Stoichiometric Constants for Binding of Acridine Orange to Calf Thymus DNA (25 °C, 0.2 M NaCl)

k_1	k_{-1}	k_2	k_{-2}	k_t	k_{-t}
$10^7\ M^{-1}\ s^{-1}$	$10^2\ s^{-1}$	$10^7\ M^{-1}\ s^{-1}$	$10^2\ s^{-1}$	$10^6\ M^{-1}\ s^{-1}$	$10^6\ M^{-1}\ s^{-1}$
3.4±0.2	2.35±0.15	1.55±0.15	5.55±0.15	1.2±0.2	8.0±0.5
n	K_1	K_2	K_t	K_I[a]	K_D[a]
	$10^5\ M^{-1}$	$10^4\ M^{-1}$		$10^5\ M^{-1}$	$10^4\ M^{-1}$
3	1.45±0.2	2.8±0.3	0.25±0.04	1.8	3.0

a) Obtained from the binding isotherm.

and $k_{-1}=235\pm15\ s^{-1}$ at 0.2 M NaCl are similar to those obtained for the intercalating dyes; $k_f \fallingdotseq 10^6\ M^{-1}\ s^{-1}$ and $k_b=50$—$7000\ s^{-1}$ for 10-methyl-9-aminoacridine, ethidium, and several phenanthridine dyes-DNA systems at 1.0 M NaCl,[26,27] $k_f=1.7\times10^7\ M^{-1}\ s^{-1}$ and $k_b=30\ s^{-1}$ for ethidium bromide-poly[d(A-T)] at 0.1 M KCl,[44] and $k_{1f}=2.2\times10^7\ M^{-1}\ s^{-1}$ and $k_{1b}=200\ s^{-1}$ for (A-T) like site[50] and $k_{2f}=3.4\times10^7\ M^{-1}\ s^{-1}$ and $k_{2b}=120\ s^{-1}$ for (G-C) like site[51] for a typical base-specific acridine dye of proflavine at 0.1 M NaCl, but not to those for the nonintercalating dye; $k_{1f}=1.5\times10^8\ M^{-1}\ s^{-1}$, $k_{1b}=5\times10^4\ s^{-1}$ and $k_{2f}=1.4\times10^8\ M^{-1}\ s^{-1}$, $k_{2b}=4\times10^3\ s^{-1}$ for di-*t*-butylproflavine-DNA system at 0.2 M NaCl.[52] Especially, the values of forward rate constants of intercalation obtained at quite similar ionic strength of 0.1 and 0.2 are quite similar each other. This may indicate that differences in the structure of dye and the base specificity are not dominant factors determining the rate of intercalation, but some specific conformational alternation of DNA helix resulting from the intercalation of dye molecule may be the rate-determining step for the intercalation process.

Externally Bound Species. The analyses of the relaxation amplitude revealed that the absorption spectrum of complex C_2 is approximately same with that of free AO molecules. Similar results were reported for the monomeric AO-polyphosphate complex.[41] Consequently, the species C_2 is reasonably attributable to an externally bound species fixed on the surface of DNA. The value of binding constant $K_2=3\times10^4\ M^{-1}$ is fairly large compared with that of electrostatic binding of acridines to the negatively charged residues of synthetic polymers ($K \fallingdotseq 10^2\ M^{-1}$).[53-55] This fact indicates that bound species C_2 is different from a simple electrostatic binding between AO and phosphate residue of DNA. Meanwhile, the rate constants $k_2=(1.55\pm0.15)\times10^7\ M^{-1}\ s^{-1}$ and $k_{-2}=(5.55\pm0.15)\times10^2\ s^{-1}$ are similar to those of other intercalating dyes rather than that of the nonintercalating dye. Accordingly, as a possible mechanism for the formation of complex C_2, we propose the partially intercalationg model adopted for the binding some acridine dyes to DNA.[56] In the present case, either one of twe dimethylamino residues of AO molecule is partially intercalating between base pairs holding the electrostatic binding of the phosphate residue of DNA ribose and the acridine ring of AO molecule is remained in the outside of DNA helix; a heavily hydrated environment around DNA helix[57] may give the absorption spectrum of AO similar to that of free AO.

As for the dimerization of AO molecule on the DNA, which is expected to occur under the condition of $r>0.1$ beyond the present experimental condition, Armstrong et al.[16] assumed that an intercalated AO molecule affords an additional binding site for free AO to form a dimerized species on DNA helix. However, this model appears suspicious from a consideration of X-ray crystallographic studies of AO-iodo CpG crystals by Reddy et al.[57] They revealed that the acridine ring of intercalated AO as well as other acridine is almost fully sandwiched between upper and lower sides of base pairs. With regard to this point, the present results would afford a better interpretation that the dimerization of AO molecules on DNA helix most likely results from a binding of free AO to an external bound species C_2, but not to an intercalative species C_1.

Magnitude of Site Exclusion Effect. Among all studies on the binding of various acridine dyes to DNA reported so far, the present study is the first study in which the value of n, a parameter indicating the magnitude of site exclusion effect, was determined kinetically.

In earlier equilibrium dialysis studies by Armstrong et al.,[16] and by Fredericq and Houssier,[17] the binding isotherm of AO-DNA system has been analyzed with $n=2$. Fornaslero and Kurucsev,[19] however, have reanalyzed the data by Armstrong et al. and pointed out that the binding isotherm in 0.1 M NaCl solution could be satisfactorily interpreted with rather $n=3$ than 2. The present result of $n=3$ in 0.2 M NaCl solution supports further the results given by Fornaslero and Kurucsev. This value ($n=3$) indicates that the three consecutive intercalation sites are blocked by one bound AO molecule. The molecular basis of this effect may be afforded by γ-kinked B DNA structure proposed by Sobell et al.[58] in their X-ray crystallographic studies of intercalating dyes-dinucleoside monophosphate crystalline complexes.

Transfer of Bound Dye between Binding Sites. One of the most important feature of the kinetic mechanism (Model III) is to involve a bimolecular pathway for direct transfer of dye molecule from one site to another. Besides the present AO-DNA system, this kind of direct transfer process has kinetically been recognized for the binding of ethidium,[26] carboxy dimidium, ethyl phenidium, desphenyl dimidium and 10-methyl-9-aminoacridine to DNA.[27] Quite recent observations by Kubota and Fujisaki suggested that proflavine and acriflavine, typical base-specific acridines, also bind to DNA via the direct transfer pathway.[59] Moreover, such transfer reactions have been demonstrated in the protein-DNA system.[60] These facts indicate that the direct transfer reaction is one of the fundamental dynamic features of DNA interaction with various ligands, and this reaction may play an important role in translocation of ligands seeking specific binding sites on DNA. Since the kinetic studies are of great advantage for elucidation of such dynamic features, extensive studies of kinetics of DNA with various kind of ligands would be required.

Finally, we should refer to kinetic models proposed for AO-DNA system by other workers. Geacintov et

al.[61] proposed by using flash photolysis technique that the intercalation takes place bimolecularly, which is consistent with the present result. However, the process of direct transfer of dye molecules was not observed in their study. This is probably because that the flash photolysis technique is insensitive to the transfer of dyes. While, Sakoda et al.[24,25] observed a single reaction step by the absorption and fluorescence stopped-flow experiments in the concentration range below 5×10^{-5} M of DNA (base pairs unit), and proposed a two-step mechanism (Model II) on the basis of the independence of the relaxation time on concentration. The values of the reciprocal relaxation times (300 s^{-1}) reported by them are in good agreement with those of the present τ_m^{-1} in the corresponding concentration range. As can be seen from Fig. 6a, however, the dependence of τ_m^{-1} on the concentration becomes remarkable at higher concentration. This facts may suggest that the stopped-flow experiments by Sakoda et al. have been done under unfavorable concentration conditions for the unambiguous elucidation of the binding mechanism.

Appendix

[A]. The cyclic reaction presented by mechanism III affords two independent rate equations. In the case that the perturbation give to the system is small, these equations can be linearized as

$$-\frac{d}{dt}\delta C_1(t) = -k_1(\bar{A}\delta S(t) + \bar{S}\delta A(t)) + k_{-1}\delta C_1(t) + k_t(\bar{S}\delta C_1(t) + \bar{C}_1\delta S(t)) - k_{-t}(\bar{S}\delta C_2(t) + \bar{C}_2\delta S(t)), \quad (A1)$$

$$-\frac{d}{dt}\delta C_2(t) = -k_2(\bar{A}\delta S(t) + \bar{S}\delta A(t)) + k_{-2}\delta C_2(t) - k_t(\bar{S}\delta C_1(t) + \bar{C}_1\delta S(t)) + k_{-t}(\bar{S}\delta C_2(t) + \bar{C}_2\delta S(t)), \quad (A2)$$

where $\delta S(t)$, $\delta A(t)$, and $\delta C_i(t)$ are the time-dependent small deviations of each reaction species from the equilibrium states after the perturbation given at $t=0$.

According to the site exclusion theory proposed by McGhee and von Hippel,[40] a function $f(r)$ represented by Eq. 10 in the text denotes the fraction of free binding site, thus

$$\bar{S}/S_0 = f(r). \quad (A3)$$

The differential of Eq. A3 affords the small deviation for S:[44]

$$\delta S(t) = f'(r)S_0\delta r(t) = f'(r)(\delta C_1(t) + \delta C_2(t)), \quad (A4)$$

where the function $f'(r)$ is the derivative of $f(r)$ (see Eq. 11 in the text). While, mass balance condition for dye requires

$$\delta A(t) = -(\delta C_1(t) + \delta C_2(t)). \quad (A5)$$

Introducing Eqs. A3, A4, and A5 into Eqs. A1 and A2, we obtain

$$-\frac{d}{dt}\delta C_1(t) = a_{11}\delta C_1(t) + a_{12}\delta C_2(t), \quad (A6)$$

$$-\frac{d}{dt}\delta C_2(t) = a_{21}\delta C_1(t) + a_{22}\delta C_2(t), \quad (A7)$$

where the coefficients a_{ij} (i, j=1 or 2) are given by Eqs. 6—9 in the text. The reciprocal relaxation times (Eqs. 4 and 5 in the text) are obtained by solving characteristic equation for the matrix $[a_{ij}]$.

[B]. The total absorbance of the solution is given by the concentration of AO in its different states and the corresponding extinction coefficients:

$$OD = \varepsilon_f\bar{A} + \varepsilon_1\bar{C_1} + \varepsilon_2\bar{C_2}. \quad (B1)$$

The time variation of the absorbance after a temperature-jump is

$$\Delta OD(t) = \varepsilon_f\delta A(t) + \varepsilon_1\delta C_1(t) + \varepsilon_2\delta C_2(t). \quad (B2)$$

A substitution of $\delta A(t)$ from Eq. A5 into Eq. B2 leads to

$$\Delta OD(t) = (\varepsilon_1 - \varepsilon_f)\delta C_1(t) + (\varepsilon_2 - \varepsilon_f)\delta C_2(t). \quad (B3)$$

The normal concentration deviations are written by linear combinations of $\delta C_1(t)$ and $\delta C_2(t)$:

$$y_i(t) = y_i^0\exp(-t/\tau_i) = \beta_i\delta C_1(t) + \delta C_2(t) \quad (B4)$$

with

$$\beta_i = (\tau_i^{-1} - a_{22})/a_{12}. \quad (B5)$$

Where the subscript i (=f, m) refers to the normal modes corresponding to the fast and middle processes, and the superscript 0 represents the value for time $t=0$. From Eq. B4, it follows

$$\delta C_1(t) = \frac{-y_f^0\exp(-t/\tau_f) + y_m^0\exp(-t/\tau_m)}{\beta_m - \beta_f}, \quad (B6)$$

$$\delta C_2(t) = \frac{\beta_m y_f^0\exp(-t/\tau_f) - \beta_f y_m^0\exp(-t/\tau_m)}{\beta_m - \beta_f}. \quad (B7)$$

Inserting Eqs. B6 and B7 into B3 yields

$$\Delta OD(t) = \Delta OD_f\exp(-t/\tau_f) + \Delta OD_m\exp(-t/\tau_m), \quad (B8)$$

with

$$\Delta OD_f = \frac{(\varepsilon_1 - \varepsilon_f) - (\varepsilon_2 - \varepsilon_f)\beta_m}{\beta_f - \beta_m}y_f^0, \quad (B9)$$

$$\Delta OD_f = \frac{(\varepsilon_1 - \varepsilon_f) - (\varepsilon_2 - \varepsilon_f)\beta_f}{\beta_f - \beta_m}y_m^0. \quad (B10)$$

As judged from Eq. B8, ΔOD_f and ΔOD_m are the amplitudes corresponding to τ_f^{-1} and τ_m^{-1}, respectively. The normal concentration, y_i^0 in Eqs. B9 and B10 can be written using the equilibrium concentrations of the actually existing reactants ans the equilitrium shifts, δK_1 and δK_2 caused by a temperature rise. From Eq. B4, the following relation is

obtained for $t=0$:

$$y_i^0 = \beta_i \delta C_1^0 + \delta C_2^0 \tag{B11}$$

According to the general procedure for the derivation of the net concentration shifts of the reacting species, we have

$$\delta C_1^0 = -\frac{f'(r)\bar{A}\bar{S}\{1 + K_2(\bar{S} - f'(r)\bar{A})\}}{1 + (K_1 + K_2)(\bar{S} + f'(r)\bar{A})}\delta K_1 + \frac{K_1 f'(r)\bar{A}\bar{S}(\bar{S} - f'(r)\bar{A})}{1 + (K_1 + K_2)(\bar{S} - f'(r)\bar{A})}\delta K_2 \tag{B12}$$

$$\delta C_2^0 = \frac{K_2 f'(r)\bar{A}\bar{S}(\bar{S} - f'(r)\bar{A})}{1 + (K_1 + K_2)(\bar{S} - f'(r)\bar{A})}\delta K_1 - \frac{f'(r)\bar{A}\bar{S}\{1 + K_1(\bar{S} - f'(r)\bar{A})\}}{1 + (K_1 + K_2)(\bar{S} - f'(r)\bar{A})}\delta K_2 \tag{B13}$$

By defining α as $\Delta H_1/\Delta H_2$ (where ΔH_1 and ΔH_2 denote the standard enthalpies in each process), δK_1 and δK_2 are connected by the relation

$$\alpha = (\delta K_1/\delta K_2)(K_1/K_2), \tag{B14}$$

If Eq. B11 is rearranged using Eqs. B12, B13, and B14, the values of y_i^0 (i=f, m) are given by the forms represented by Eq. 16 in the text.

References

1) F. H. C. Crick, L. Barnett, S. Brenner, and R. J. Watts-Tobin, *Nature (London)*, **192**, 1227 (1961).

2) S. Brenner, L. Barnett, F. H. C. Crick, and A. Orgel, *J. Mol. Biol.*, **3**, 121 (1961).

3) N. Yamamoto, *J. Bacteriol.*, **75**, 443 (1958).

4) A. Albert, "Selective Toxicity," 2nd ed, Champman & Hall, London (1973).

5) J. Ciak and F. E. Hahn, *Science*, **156**, 655 (1967).

6) A. Blake and A. R. Peacocke, *Biopolymers*, **6**, 1225 (1968).

7) E. F. Gale, E. Cundliffe, P. E. Reynolds, M. H. Richmond, and M. J. Waring, "The Molecular Basis of Antibiotic Action," Wiley, New York (1972).

8) N. C. Seeman, R. O. Day, and A. Rich, *Fed. Proc., Fed. Am. Soc. Exp. Biol.*, **33**, 1537 (1974).

9) C. Tsai, S. C. Jain, and H. M. Sobell, *J. Mol. Biol.*, **114**, 301 (1977).

10) S. C. Jain, C. Tsai, and H. M. Sobell, *J. Mol. Biol.*, **114**, 317 (1977).

11) H. M. Sobell, C. Tsai, S. C. Jain, and S. G. Gilbert, *J. Mol. Biol.*, **114**, 333 (1977).

12) S. Neidle, A. Achari, G. L. Taylor, H. M. Berman, H. L. Carrell, J. P. Glusker, and W. C. Stalling, *Nature (London)*, **269**, 304 (1977).

13) A. R. Peacocke and J. N. H. Skerrett, *Trans. Faraday Soc.*, **52**, 261 (1956).

14) J. Chambron, M. Daune, and C. H. Sadron, *Biochim. Biophys. Acta*, **123**, 306 (1966).

15) S. Ichimura, M. Zama, H. Fujita, and T. Ito, *Biochim. Biophys. Acta*, **190**, 116 (1970).

16) R. W. Armstrong, T. Kurucsev, and U. P. Strauss, *J. Am. Chem. Soc.*, **92**, 3174 (1970).

17) E. Fredericq and C. Houssier, *Biopolymers*, **11**, 2281 (1972).

18) Y. Kubota, Y. Eguchi, K. Hashimoto, M. Wakita, Y. Honda, and Y. Fujisaki, *Bull. Chem. Soc. Jpn.*, **49**, 2424 (1976).

19) D. Fornaslero and T. Kurucsev, *J. Phys. Chem.*, **85**, 613 (1981).

20) M. J. Waring, *J. Mol. Biol.*, **13**, 269 (1965).

21) L. M. Chan and Q. Van Winkle, *J. Mol. Biol.*, **40**, 491 (1969).

22) S. Tanaka, Y. Baba, A. Kagemoto, and R. Fujishiro, *Makromol. Chem.*, **181**, 2175 (1980).

23) H. J. Li and D. M. Crothers, *J. Mol. Biol.*, **39**, 461 (1969).

24) M. Sakoda, K. Hiromi, and K. Akasaka, *Biopolymers*, **10**, 1003 (1971).

25) M. Sakoda, K. Hiromi, and K. Akasaka, *J. Biochem.*, **71**, 891 (1972).

26) J. L. Breslofe and D. M. Crothers, *J. Mol. Biol.*, **95**, 103 (1975).

27) L. P. G. Wakelin and M. J. Waring, *J. Mol. Biol.*, **144**, 183 (1980).

28) R. K. Tubbs, W. E. Ditmars Jr., and Q. Van Winkle, *J. Mol. Biol.*, **9**, 545 (1964).

29) J. C. Thomes, G. Weill, and M. Daune, *Biopolymers*, **8**, 647 (1969).

30) N. F. Ellerton and I. Isenberg, *Biopolymers*, **8**, 767 (1969).

31) B. Weisblum and P. L. de Haseth, *Proc. Natl. Acad. Sci. U. S. A.*, **69**, 629 (1972).

32) Y. Kubota, *Chem. Lett.*, **1973**, 299.

33) J. P. Shreiber and M. P. Daune, *J. Mol. Biol.*, **38**, 487 (1974).

34) S. A. Latt, S. Brodie, and S. H. Munroe, *Chromosoma*, **49**, 17 (1974).

35) Y. Kubota and R. F. Steiner, *Biophys. Chem.*, **6**, 279 (1977).

36) S. Georghion, *Photochem. Photobiol.*, **22**, 103 (1975).

37) G. Weill and M. Calvin, *Biopolymers*, **1**, 401 (1963).

38) A. L. Stone and D. F. Bradley, *J. Am. Chem. Soc.*, **83**, 3627 (1961).

39) S. Inoue, Y. Toyoshima, and T. Yasunaga, *J. Phys. Chem.*, **85**, 1401 (1981).

40) J. D. McGhee and P. H. von Hippel, *J. Mol. Biol.*, **86**, 469 (1974).

41) D. F. Bradley and M. K. Wolf, *Proc. Natl. Acad. Sci. U. S. A.*, **45**, 944 (1959).

42) B. J. Gardner and S. F. Mason, *Biopolymers*, **5**, 79 (1967).

43) M. Zama and S. Ichimura, *Biopolymers*, **9**, 53 (1970).

44) T. M. Jovin and G. Striker, *Mol. Biol. Biochem. Biophys.*, **24**, 245 (1978).

45) D. E. V. Schmechel and D. M. Crothers, *Biopolymers*, **10**, 465 (1971).

46) N. Harada and K. Nakanishi, *Acc. Chem. Res.*, **5**, 257 (1972).

47) R. B. Gennis and C. R. Cantor, *J. Mol. Biol.*, **65**, 381 (1972).

48) A. Chan, R. Kilkuskie, and S. Hanlon, *Biochemistry*, **18**, 84 (1979).

49) D. J. Patel, S. A. Kozlowski, J. W. Suggs, and S. D.

Cox, *Proc, Natl. Acad. Sci. U. S. A.*, **78**, 4063 (1981).

50) The binding of proflavine to (A-T) sites was analyzed according to a two-step mechanism, and the first-order forward rate constant ($3.3\times10^3\ s^{-1}$) was given in the literature.[51] In order to facilitate the comparison with other systems, the product of this value and the equilibrium constant for the preequilibrium ($6.6\times10^3\ M^{-1}$), which provides the apparent second-order rate constant for the intercalation, was cited in this paper.

51) J. Ramstein, M. Ehrenverg, and R. Riyler, *Biochemistry*, **19**, 3938 (1980).

52) W. Muller, D. M. Crothers, and M. J. Waring, *Eur. J. Biochem.*, **39**, 223 (1973).

53) G. Schwarz, S. Klose, and W. Balthasar, *Eur. J. Biochem.*, **12**, 454 (1972).

54) G. Schwarz and W. Balthasar, *Eur. J. Biochem.*, **12**, 461 (1972).

55) G. Schwarz and S. Klose, *Eur. J. Biochem.*, **29**, 249 (1972).

56) P. S. Drummond, V. F. W. Simpson, and A. R. Peacocke, *Biopolymers*, **3**, 135 (1965); H. Ushio, *J. Sci. Hiroshima Univ., Ser. A*, **41**, 209 (1977).

57) B. S. Reddy, T. P. Seshadri, T. D. Sakore, and H. M. Sobell, *J. Mol. Biol.*, **135**, 787 (1979).

58) H. M. Sobell, C. Tsai, S. G. Jain, and S. G. Gilbert, *J. Mol. Biol.*, **114**, 333 (1977).

59) Y. Kubota and Y. Fujisaki, unpublished results.

60) D. M. Crothers and M. Fried, *Cold Spring Habor Symp. Quantum Biol.*, **47**, 263 (1983).

61) N. E. Geacintov, J. Waldmeyer, V. A. Kuzmin, and T. Kolubayev, *J. Phys. Chem.*, **85**, 3608 (1981).